

Removal of Phosphorus from Water onto Marsh Clam Shell to Predict Contour for Removal Efficiency and Mass of Adsorbent

Nur Husna Muslim^{a*}, Akmal Danial Mohd Faizal^b, Muhamad Amir Syahmi Sophian^b, Muhammad Amir Firdaus Abd Rashid^b, Noorul Hudai Abdullah^{b*}, Norzainariah Abu Hassan^{a,c} & Nur Atikah Abdul Salim^d

^a*Faculty of Engineering Technology, Universiti Tun Hussein Onn Malaysia, Hab Pendidikan Tinggi Pagoh, Km 1, Jalan Panchor, 84600 Muar, Johor, Malaysia.*

^b*Neo Environmental Technology, Centre for Diploma Studies, Universiti Tun Hussein Onn Malaysia, Pagoh Education Hub, 84600 Pagoh, Johor, Malaysia*

^c*Department of Civil Engineering, Politeknik Melaka, No. 2, Jalan PPM10, Plaza Pandan Malim 75250 Melaka, Malaysia Faculty of Engineering & Built Environment, Universiti Kebangsaan Malaysia, Malaysia*

^d*School of Occupational, Safety & Health, Netherlands Maritime University College, Johor Bahru, Johor, 80000 Malaysia*

*Corresponding author: noorul@uthm.edu.my & nurhusnabintimuslim@gmail.com

Received 23 July 2024, Received in revised form 24 October 2024
 Accepted 24 November 2024, Available online 30 January 2025

ABSTRACT

Anthropogenic activities have resulted in considerable water quality degradation in water sources due to a common problem of the excessive nutrient content (phosphorus) in receiving water, resulting in eutrophication. Even though various wastewater treatment methods have been applied, focusing on phosphorus removal through biological, physical, and chemical treatment, there is still a need to identify the eco-friendly method using the adsorption process and verify the theoretical and experimental data via kinetic and isotherm models. Hence, this study investigates phosphorus removal efficiency from water onto raw marsh clam shells and verifies the experimental and theoretical data with kinetic and isotherm studies. The variable of this study used different masses (2, 4, 6, 8, 10 g) of adsorbents with particle sizes from 1.18 mm to 2.36 mm to remove phosphorus from an aqueous solution (5 mg/L). The physical-chemical properties of adsorbents were examined using X-ray diffraction (XRD), scanning electron microscopy (SEM), Energy Dispersive X-ray Fluorescence (EDXRF), and Fourier Transform Infrared Spectroscopy (FTIR) to support the experimental data and identify the possibility of phosphorus adsorption. The batch experiment data obtained were verified using the kinetic (pseudo-first-order and pseudo-second-order) and isotherm (Langmuir and Freundlich) models. The experiments showed that the best contact time for all masses was 1440 min and the best adsorbent dose was 10 g with 78.0% removal. By comparing the two adsorption isotherm models, the study finds that the adsorption isotherm fits the Langmuir isotherm model with a correlation coefficient, R^2 of 0.9006. The novel use of adsorbent marsh clam shell as a potential adsorbent in the application of future water treatment technologies.

Keywords: Adsorption; phosphorus; kinetic; isotherm; marsh clam shell

INTRODUCTION

Eutrophication is the main environmental issue impacting water resources and aquatic ecosystems. It is to blame for the degradation of water quality and extremely restricts

water consumption. Eutrophication is brought on by humans oversupplying water bodies with nutrients, particularly phosphorus (Beretta-Blanco & Carrasco-Letelier 2021). The dissolved oxygen concentration in the lower layer of a stratified lake or reservoir deficiency can lead to eutrophic conditions due to the vast amount of

organic matter produced by algal blooms, which cannot fully degrade while increasing the levels of dangerous reduced compounds, with the production of foul aromas and tastes.

The 90 largest lakes in Malaysia are more than 60% eutrophic (Sharip et al. 2014). The standard phosphate concentration allowed for Standard B effluent in the Second Schedule (Jiménez, 2005) is 10 mg/L. This value is relatively high compared to other countries, such as Japan, which only allows a phosphate concentration of 1 mg/L (Mulkerrins et al. 2004). When water bodies age, eutrophication causes algal blooms and the extinction of aquatic species (Alkurdi et al. 2021). The most dangerous result of eutrophication is an excess of phytoplankton biomass, particularly cyanobacterial blooms (Feng et al. 2023). These blooms put aquatic animals at risk of hypoxia or anoxia at night, cast a shadow over submerged aquatic plants, and endanger wildlife, domestic animals, and people due to the toxins some cyanobacteria species emit.

Besides, the primary cause of eutrophication is phosphorus, mostly produced by human activity. Nitrogen and phosphorus are essential to plant nutrients in fertilisers used in agricultural pursuits like gardening. Our homes are to blame for the phosphate pollution in the wastewater. Several cases of phosphate pollution have been recorded in the last 10 years. These events occurred near populated regions, showing that human activity is one of the main drivers of phosphate pollution (Xiong et al. 2011). In addition, common sources of phosphate include cleaning supplies like dish soap, laundry soap, and car shampoo, all of which are simple to remove without considering the effects.

There are several processes commonly used in treating phosphorus in water and wastewater: chemical precipitation, biological phosphorus removal and adsorption. This study focuses on adsorption involves using a medium to attract and bind phosphorus from the water or wastewater. The medium adsorbs the phosphorus onto its surface, effectively removing it from the water. The medium can be regenerated or replaced when it becomes saturated with phosphorus. Adsorption of phosphorus from wastewater using marsh clam shells can be an effective method due to the high calcium carbonate content in the shells, which has the ability to adsorb phosphorus ions (Boeykens et al. 2017).

Many adsorbents have been used for phosphate removal from water, including chitosan (Oktor et al. 2023), silica nanoparticles (Nguyen, 2022), volcanic rocks (Mekonnen et al. 2021), bottom ash (Hashim et al. 2021) and pumice (Fetene & Addis, 2020). This study using marsh clam shells as an adsorbent, where promising adsorbent to recover phosphate from wastewater, making them helpful for wastewater treatment systems. This is a good chance to employ mussel shells as an adsorbent for phosphate

since they are obtainable freely at no cost and have the potential to adsorb phosphate in solutions (Mishra et al. 2022). Even though this study creates contour predictions for removal efficiency and mass of adsorbent to facilitate the industrial use of contours to estimate removal efficiency using appropriate adsorbent mass, it can confirm the results using kinetics and isotherms. The purposes of this study are (1) to investigate the removal efficiency of phosphorus from water onto raw marsh clam shell, (2) to verify the experimental and theoretical data with kinetic and isotherm studies, and (3) to develop the prediction contour for removal efficiency and mass of adsorbent and prove that the shell of the marsh clam shell is a very effective adsorbent to remove phosphate.

MATERIALS & METHODS

The marsh clamshell samples were acquired from Bachok, Kelantan, Malaysia. The samples were cleansed with tap water and dried under sunlight, followed by placing in an oven for 2 days at 30 °C to completely dry. The adsorbent was ground before being sieved to 1.18 mm – 2.36 mm particle sizes. This particle size range was chosen based on previous study which indicates that particles within this range provide an optimal surface area (Abdullah et al. 2024). If smaller particles were used, the increased surface area could enhance adsorption but may cause filtration and separation (Hussein et al. 2024). Meanwhile, larger particles with less surface area may reduce adsorption capacity and slow the kinetics (Jing et al. 2024). Hence, the selected range size optimizes adsorption while ensuring practical handling. The synthetic solution (i.e., 100 mg/L) was prepped by solubilizing Potassium dihydrogen phosphate (KH_2PO_4) with the weight amount of 0.1433 g into 1 L of deionized water in a volumetric flask. The synthetic solution was diluted with deionized water to obtain the specified concentration of 5, 10, 15, 20, 25 mg/L.

The batch experiments were performed to identify the adsorption isotherm and kinetic. The kinetic analyses were performed by inserting 2, 4, 6, 8, and 10 g of the adsorbent into an Erlenmeyer flask. Every flask contained 0.1 L of either synthetic solution with a 5 mg/L of PO_4^{3-} concentration, respectively. Acknowledge that the concentration of phosphorus in the synthetic solution for the adsorption of a single solute was updated to have the similar concentration as those validated in the domestic wastewater treatment from a previous study for the adsorption of various solutes (Kesari et al. 2021). Every solution sample was agitated from 1 to 4 days at 170 rpm, and the PO_4^{3-} concentrations in every flask were identified at specific time intervals until the adsorbent was saturated.

The solution samples were filtered, and the PO_4^{3-} concentrations in every flask were analyzed by utilizing the HACH DR 6000 UV-Vis Spectrophotometer.

The pseudo-first-order and pseudo-second-order models were implemented to comprehend the kinetics of phosphorus adsorption onto Marsh Clam Shell from either the synthetic solution. Freundlich and Langmuir isotherm models were implemented to determine the adsorption

isotherms of phosphorus for the synthetic solution. The prediction of contour to estimate the removal of efficiency of phosphorus from water with different initial concentrations and mass of adsorbent needed was developed from the batch experiment using initial phosphorus concentrations of 5, 10, 15, 20, and 25 mg/L mixing with 2, 4, 6, 8, 10 g for 4 days, as illustrated in Figure 1.

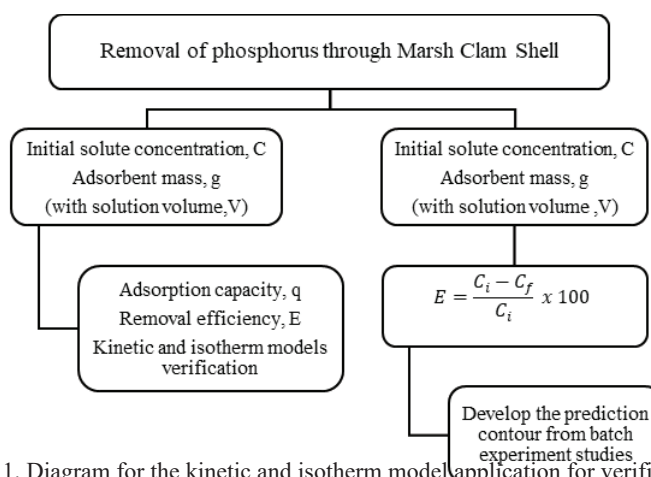


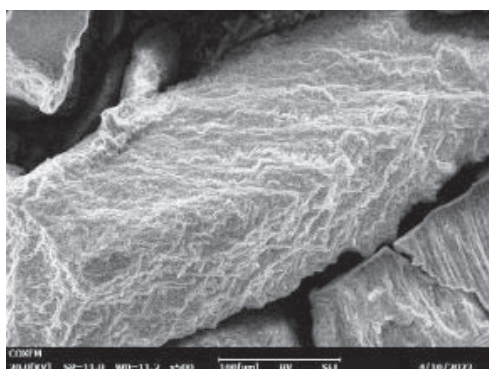
FIGURE 1. Diagram for the kinetic and isotherm model application for verification of the adsorption process

RESULTS AND DISCUSSION

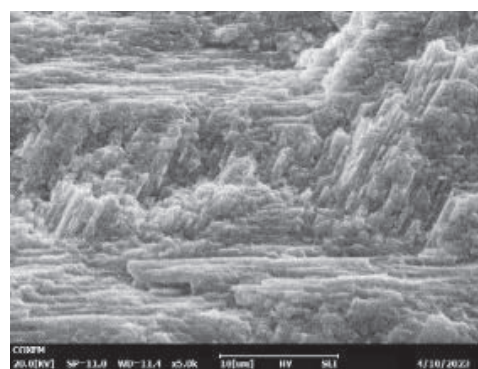
CHARACTERISTICS OF THE ADSORBENT

Physicochemical properties of marsh clam shells, such as EDXRF, SEM, and FTIR, were investigated. Phosphate adsorption onto raw marsh clam shells and calcined marsh clam shells was described using the kinetic and isotherm model. Analysis using EDXRF, SEM, XRD, and FTIR

revealed the characteristics of raw marsh clam shells. Figure 2 displays the marsh clam shells' surface under SEM magnifications of 500, 2500, and 5000 times. Figures 2 (a), (b), and (c) demonstrate the uneven, rough, and porous surface structure of the raw marsh clam shells. Figure 1(c) shows the homogeneous porosity of marsh clam shells surface with high content of Ca and O to adsorb phosphate in solution under 5000 times magnification. While Figure 2 (d), (e), and (f) indicates the marsh clam shells' porous surface after the adsorbent happened.



(a)



(b)

continue ...

... cont.

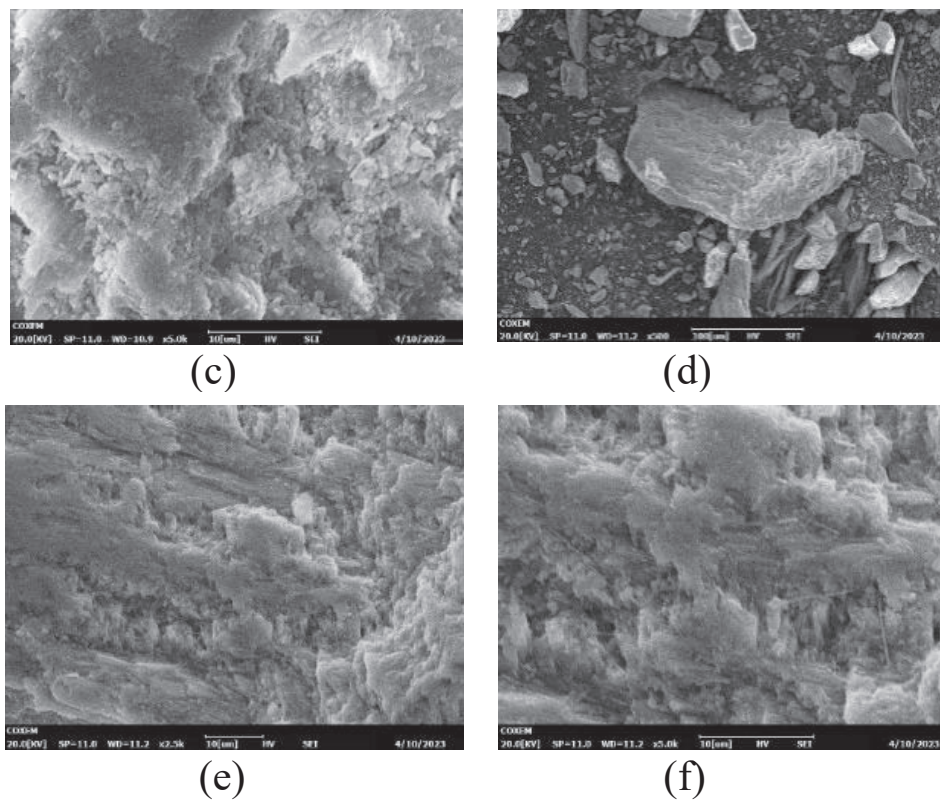


FIGURE 2. The SEM photomicrograph of raw marsh clam shells before adsorption are (a), (b), and (c), while after adsorption, are (e), (f), and (g) with magnifications of 500, 2500, and 5000.

Table 1 shows the composition of the raw marsh clam shell before and after adsorption. The major composition before adsorption was identified as Ca (72.86%) and C (23.73%), while the minor composition was Fe (2.02%)

and Al (1.39%). After adsorption, the major composition was identified as Ca (49.95%) and C (48.33%), while Fe (1.48%) and Al (0.24%) have been identified as the minor composition.

TABLE 1. Elemental composition of the raw marsh clam shell for (a) before adsorption and (b) after adsorption

Element	Weight (%)	
	Before	After
Ca	72.86	49.95
Fe	2.02	1.48
Al	1.39	0.24
C	23.73	48.33
Total	100.00	100.00

The Fourier Transform Infrared (FTIR) was implemented to detect the chemical bonds in the raw marsh clam shell by creating an infrared absorption spectrum. The electromagnetic radiation spectrum's infrared area can be measured with its assistance. In this instance, the

phosphate was absorbed using the marsh clam shell as an adsorbent. Prior to the absorption procedure, the FTIR reading was 2067.40 , 2011.36 , 1471.12 , and 861.83 respectively. The outcomes following absorption showed that after the adsorption, the reading is 2085.22 cm^{-1} , 2026.97 cm^{-1} for -NCS and non for the C-O class group.

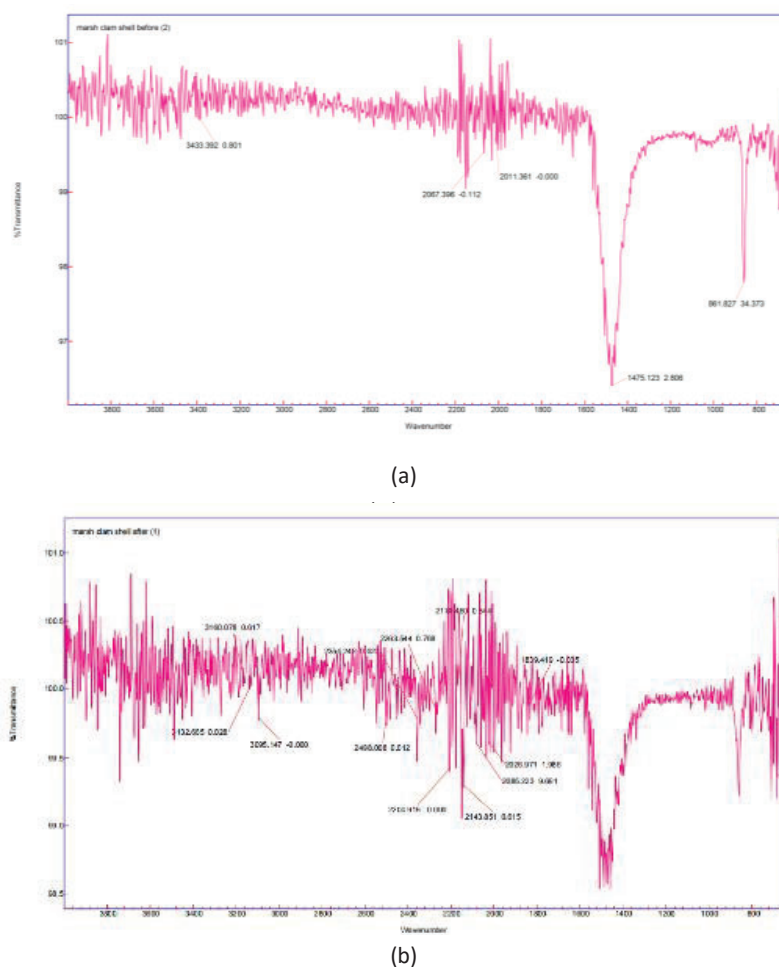


FIGURE 3. FTIR spectra of the raw marsh clam shell, (a) before and (b) after adsorption

TABLE 2. Function group of FTIR spectra of raw marsh clam shell before and after adsorption

Frequency spectrum (cm^{-1})			Functional Group Class	References
Before Adsorption	After Adsorption	Differences		
2067.40	2085.22	17.83	-NCS	Coates, 2000
2011.36	2026.97	15.61	-NCS	Coates, 2000
1471.12	-	-	C-O	Wu et al. 2017
861.83	-	-	C-O	Kim et al. 2018

The effect of the phosphorus molecules adsorbed onto the marsh clam shell surface on isothiocyanate ($-\text{NCS}$) bending may rise until 17.83 cm^{-1} (2085.22 cm^{-1}) and 15.61 cm^{-1} (2026.97 cm^{-1}) frequency spectrum due to ion exchange Isothiocyanate functional group. The condition may influence the stretching due to the vibrations (Ebrahiminezhad et al. 2013). After the adsorption of phosphorus solute from synthetic solution onto the marsh clam shell, an additional peak detected at 1471.12 cm^{-1} was discovered and could be assigned to the C-O stretching

vibration onto the marsh clam shell surface, indicating isothiocyanate was generated (Wu et al. 2017).

Lastly, the XRD analysis shows the surface composition of carbonate minerals on the adsorbent before and after the adsorption process. From the XRD analysis, as in Figure 4, the carbonate mineral (Aragonite) contained in the adsorbent is 100%. After 3 days of the adsorption progress, the percentage of calcite on the adsorbent increased to 13%, and Aragonite reduce to 87% due to reaction on phosphorus in water as indicated in Figure 4.

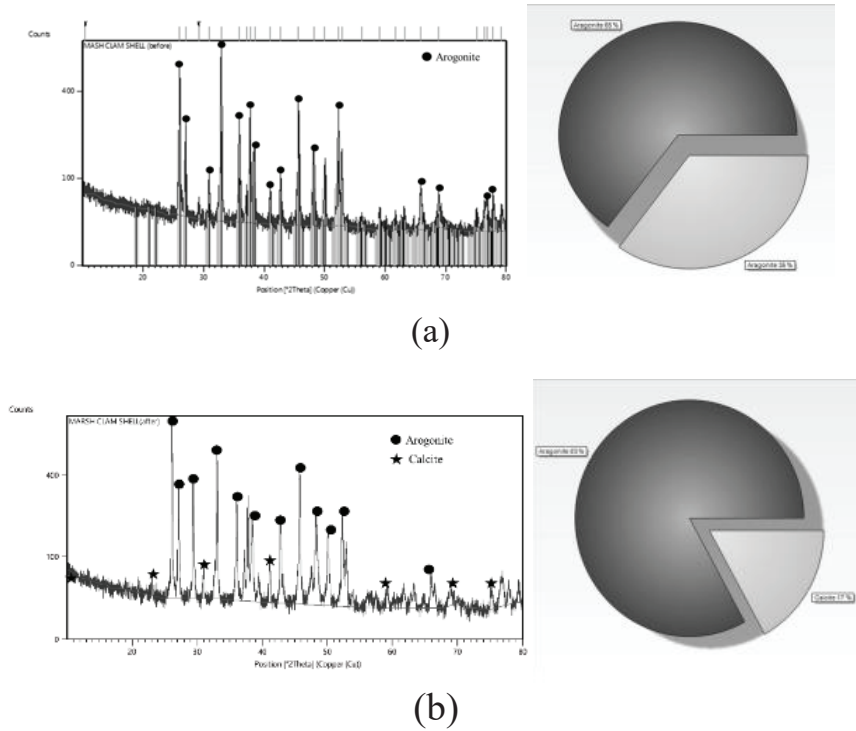


FIGURE 4. XRD pattern and composition of (a) before, (b) after phosphorus adsorption process for raw marsh clam shells

ADSORPTION CAPACITY, Q AND REMOVAL EFFICIENCY, E OF PHOSPHORUS

To determine the phosphorus concentrations in marsh clam shells, the equilibrium-corresponding contact period was calculated by tracking the rate of phosphorus adsorption on marsh clam shells over time (Tan et al. 2023). This is done to evaluate the correlation between adsorption uptake monitoring over time at a specific concentration and adsorption kinetics, which measures the amount of diffusion adsorbate that contacts pores (Luo et al. 2023). The initial few minutes may be characterized as the speed of adsorption kinetic existence in a significant quantity due to the surface of active sites exist at the beginning of the adsorption and those that remain after a given amount of time. Adsorption is the transition from liquid to solid phase.

The amount of adsorbate adsorbed per unit mass defines adsorption capacity performance. Adsorption capability, or the potential of adsorption for every mass of particle, refers to the overall value of the marsh clam shells employed in this study to adsorb phosphorus from wastewater. The adsorption capacity was calculated as (1).

$$q = \frac{C_i - C_f}{m} \times V \quad (1)$$

where, C_i represents initial concentration of phosphorus, C_f is the final concentration of phosphorus, m expresses the mass of adsorbent and V represents adsorbent volume.

The performance of the adsorption capacity for five different marsh clam shells particle masses is illustrated in Figure 5. At 1440 min, the capacity of adsorption for each mass of particles reached an equilibrium state, and it stayed constant for the next 4320 min. The equilibrium adsorption capacity, q_e are 0.1175 mg/g (2 g), 0.0813 mg/g (4 g), 0.0603 mg/g (6 g), 0.0603 mg/g (8 g), and 0.0499 mg/g (10 g) for each mass of the particles. This means that although it took a while to reach an equilibrium state with this particle size, it exhibits good removal effectiveness once the adsorption process is complete. The kinetic and isotherm models depend on the equilibrium state's adsorption capability.

The effectiveness of the adsorbent for the phosphorus removal from synthetic wastewater was also determined. The removal efficiency, E (%), was calculated using as equation (2).

$$E = \frac{C_i - C_f}{C_i} \times 100\% \quad (2)$$

The relationship between removal efficiency and contact time is seen in Figure 5(a). The rapid progress of adsorbate occupying the vacant sites on the adsorbent's porous surface until equilibrium was approached when all the vacant sites were completely occupied is demonstrated by the rapid increase in removal efficiency as the contact duration rises (Penn et al. 2017). The highest removal efficiencies for each particle mass were 36.7% (2 g), 50.8% (4 g), 56.6% (6 g), 75.3% (8 g), and 78.0% (10 g). It was discovered that the removal efficiency rises with time. The marsh clam shells size 1.18 mm showed the best removal performance (72.97%), followed by size 0.075 mm with 67.34% phosphate adsorbed during the past study (Abdullah et al. 2023). The correlation of the best removal efficiency against the mass of adsorbent was made using the equilibrium adsorption capacity, q_e , and removal efficiency, E , relationship. The pattern shows that the adsorption capacity decreases as the removal efficiency rises, which implies that the progress of adsorption at active sites accelerates (Abdullah et al. 2023), as shown in Figure 6(b).

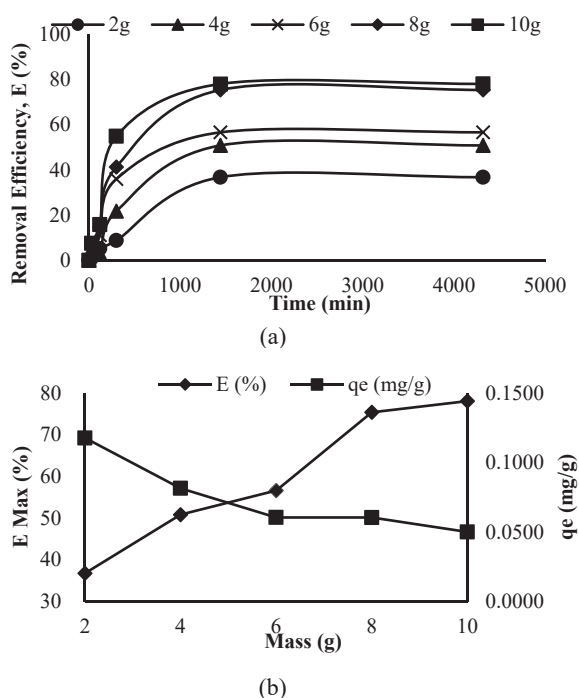


FIGURE 5. The implementation of removal efficiency, E (%) with time, t (min) for the mass of adsorbent, and (b) correlation of removal efficiency, E (%) and adsorption capacity, q (mg/g) towards mass(g)

PSEUDO-FIRST-ORDER AND PSEUDO-SECOND-ORDER KINETIC MODEL

The pseudo-first-order and pseudo-second-order kinetic models were implemented to analyze the process of adsorption. Chemical kinetics uses the term “Pseudo First Order reaction” to designate a specific kind of non-first-order reaction. The concentration of the reactant falls at a rate proportional to the concentration of the reactant raised to some power in this simplified model, which is frequently implemented to describe the kinetics of chemical reactions (Revellame et al. 2020). The pseudo-first-order can be calculated using equation (3).

$$\ln(q_e - q_t) = \ln q_e - k_1 t \quad (3)$$

where q_e is the equilibrium amount of phosphorus adsorbed, q_t is the amount of phosphorus adsorbed at a time, k_1 is the constant rate of pseudo-first-order equations, and t is the time of adsorption.

F_e values were calculated for both models. With the aim of evaluating which model is the best to define the adsorption kinetic with the highest and least F_e , the values for the two models were determined and compared. The formula for F_e is shown in (4).

$$F_e = \sqrt{\left(\frac{1}{n-p}\right) \sum_i^n (q_{t(\text{exp})} - q_{t(\text{theo})})^2} \quad (4)$$

The number of measurements is represented by n , the number of kinetic parameters is represented by p , and the experimental and theoretical adsorption capacities are represented by $q_{t(\text{exp})}$ and $q_{t(\text{theo})}$. The pseudo-second-order kinetic model predicts the behavior across the whole adsorption range, which predicts that chemical sorption or chemisorption is the rate-limiting phase. In this instance, the adsorption rate is determined by adsorption capacity rather than adsorbate concentration.

Referring to the concept that chemical sorption or chemisorption is the rate-limiting phase, the pseudo-second-order kinetic model assumes behavior across the whole adsorption range. In this case, adsorption capacity rather than adsorbate concentration determines the adsorption rate as equation (5).

$$\frac{t_i}{q_t} = \frac{1}{k_2 q_e^2} + \frac{t_i}{q_e} \quad (5)$$

where, q_t is the quantity of absorption at t time, q_e is the equilibrium absorption amount, and k_2 is the pseudo-second-order constant.

Figure 6(a) illustrates linear regression analysis for the pseudo-first-order model and Figure 6(b) pseudo-second-order for the adsorption of phosphorus onto marsh clam shell from aqueous solution. From Figure 6, the pseudo-first-order model has the highest R^2 (0.9951) compared to R^2 from the pseudo-second-order model (0.9889). This means the pseudo-first-order model is a better kinetic model to capture adsorption kinetic due to its highest adsorption rate. In comparison to the previous study, the pseudo-second-order model is higher than the pseudo-first-order model (Abdullah et al. 2024). Table 3 shows that 6 g and 8 g have the same adsorption capacity and different removal efficiency, which are ($R^2=0.9725$ and 0.9951) and Fe (0.0288 and 0.0239). While the particle mass of 2 g has a high adsorption capacity but poor removal

efficiency, with R^2 (0.9602) and Fe (0.0308) for the pseudo-first-order model.

Table 3 shows that all adsorbent masses for Pseudo-Second-Order have an excellent coefficient correlation close to 1. However, among all masses, the mass of adsorbent for 10 g has the highest (0.9889), suggesting the highest adsorption rate. It has been determined that the pseudo-first-order model, whose highest R^2 (0.9951) is higher than the pseudo-second-order model's R^2 (0.9889), indicates a better kinetic model to capture adsorption kinetics. Additionally, the F_e of the pseudo-second-order model is higher (0.0860) than the pseudo-first-order model's (0.0154). This proves unequivocally that the data fit the pseudo-first-order model greater than the pseudo-second-order model. This means that in this study, pseudo first order model showed greater results in phosphorus adsorption than the pseudo-second-order model.

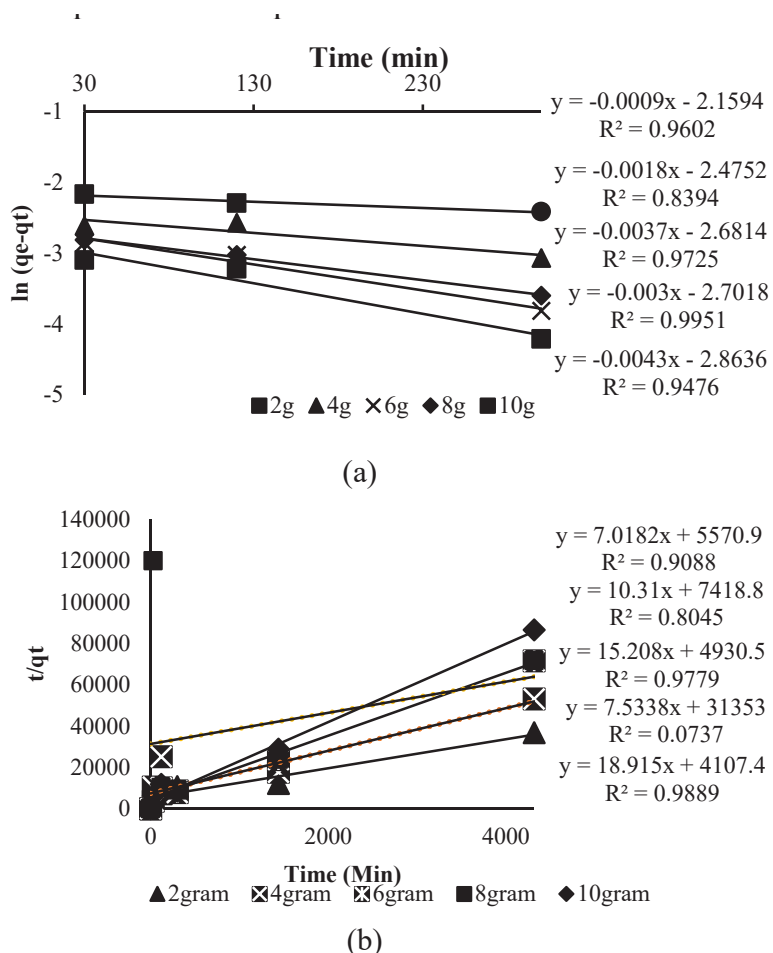


FIGURE 6. Kinetic models of (a) pseudo-first-order and (b) pseudo-second-order analysis for the adsorption of phosphorus onto adsorbent from aqueous solution

ADSORPTION FREUNDLICH AND LANGMUIR ISOTHERM MODEL

The simultaneous adsorption of cation and anion on the same surface of an adsorbent is the foundation of the Freundlich isotherm model. The Freundlich isotherm model, which is based on multilayer adsorption, defines

adsorption processes on heterogeneous surfaces and active sites. An empirically grounded model is the Freundlich isotherm (García-Zubiri et al. 2009). In this model, C_e represents the equilibrium concentration, and q_e denotes the amount of adsorbate per unit of adsorbent at equilibrium (measured in mg/g). The adsorbent and adsorbate affect the parameters and n , as shown in equation (6).

TABLE 3. Kinetic parameter of pseudo-first-order and pseudo-second-order model

Kinetic Models	Mass (g)	$q_{e(\text{theo})}$ (mg/g)	k_1 (/min)	R^2	F_e	$q_{e(\text{exp})}$ (mg/g)
Pseudo-First-Order	2	0.1154	0.0009	0.9602	0.0308	0.1175
	4	0.0841	0.0018	0.8394	0.0154	0.0813
	6	0.0685	0.0037	0.9725	0.0288	0.0603
	8	0.0671	0.0030	0.9951	0.0239	0.0603
	10	0.0571	0.0043	0.9476	0.0252	0.0499
Kinetic Models	Mass (g)	$q_{e(\text{theo})}$ (mg/g)	k_2 (/min)	R^2	F_e	$q_{e(\text{exp})}$ (mg/g)
Pseudo-Second-Order	2	0.1424	0.0088	0.9088	0.5270	0.1175
	4	0.0969	0.0066	0.8045	0.4240	0.0813
	6	0.0657	0.0100	0.9779	0.7300	0.0603
	8	0.1327	0.0016	0.0737	0.0860	0.0603
	10	0.0528	0.0120	0.9889	0.9190	0.0499

$$q_e = K_f C_e^{1/n} \quad (6)$$

The temperature-dependent constant and can be determined using linear regression when the equation is linearised as (7) for the Freundlich isotherm model.

$$\ln q_e = \ln K_f - \frac{1}{n} \ln C_e \quad (7)$$

A thermodynamic model known as the Langmuir isotherm describes the sorption of substances on a solid's surface. It is assumed that the solid's surface is homogeneous and has a finite number of identical spots that can each contain one sorbate molecule (Shimazu & Matubayasi, 2023). According to the Langmuir isotherm equation, the sorption rate is proportionately related to the difference between the concentration of sorbate adsorbed on the surface of the solid and the concentration of sorbate in the liquid phase. The amount of sorbate adsorbed at equilibrium is also directly proportional to the sorbate concentration in the liquid phase. The equation for Langmuir is used as (8).

$$\frac{1}{q_e} = \frac{1}{K_L q_{max} C_e} + \frac{1}{q_{max}} \quad (8)$$

The correlation coefficients represented by and the Langmuir and Freundlich adsorption constants are shown in Figure 7. The findings were adjusted using the Langmuir isotherm models to identify the best model for the adsorption of metal ions., where the Langmuir isotherm model (= 0.9392) is higher than the Freundlich model (= 0.9006). This indicates that the rate of adsorbent in the Langmuir model is higher than the Freundlich model.

The adsorption of phosphorus onto raw marsh clam shells fitted to the Langmuir Model. All the parameter values derived using isotherm models are indicated in Table 3. The findings show that marsh clam shells can absorb phosphorus from synthetic solutions. This is because the phosphate ions and the calcium oxide, which is 65% on the surface of marsh clam shells, strongly attract one another due to their different charges.

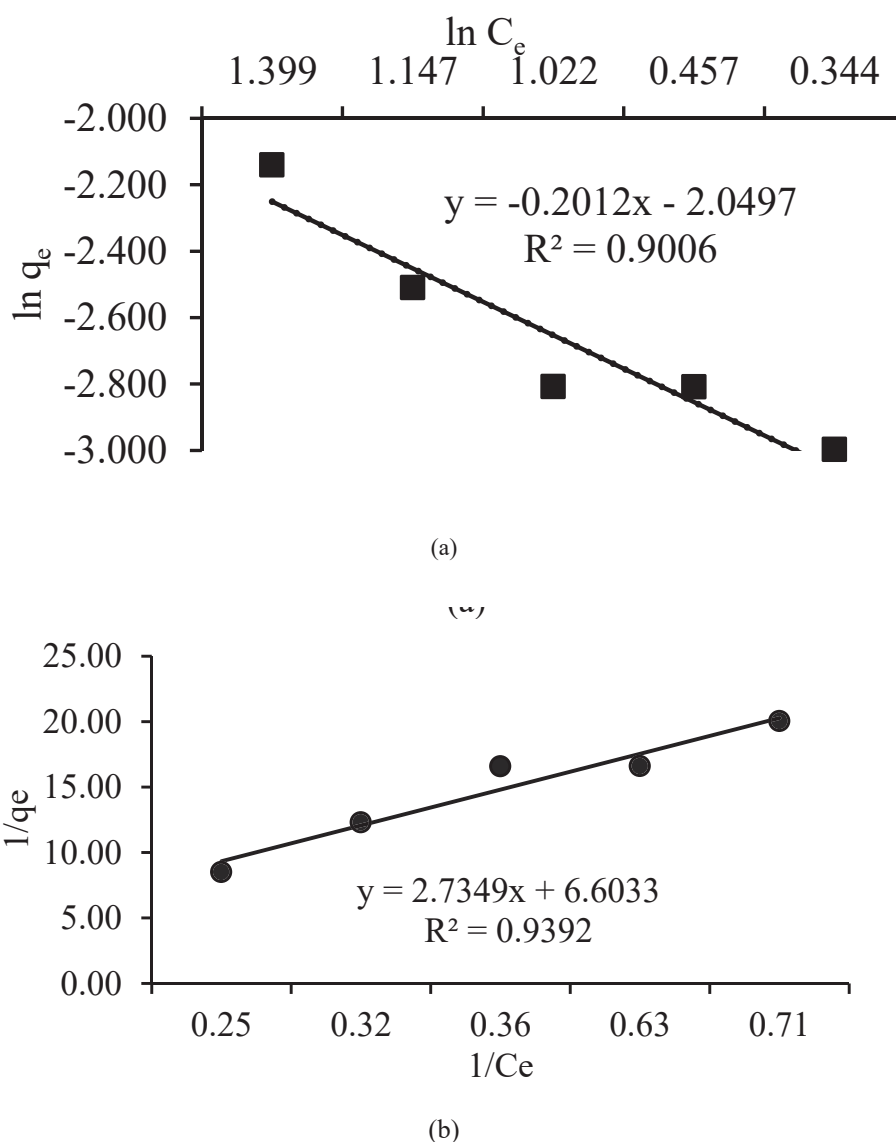


FIGURE 7. Linear plot of (a) Freundlich model of $\ln(C_e)$ against $\ln(q_e)$, and Langmuir model of $1/q_e$ against $1/C_e$.

TABLE 4. Freundlich and Langmuir of the Isotherm Model Parameters

Freundlich model			Langmuir model		
n	K_F (mg/g)	R^2	q_{max} (mg/g)	K_L (mg/g)	R^2
-4.9701	0.1296	0.9006	6.6033	0.05676	0.9392

The quantities represent Freundlich constants for the adsorption capacity and intensity, and n , respectively. By plotting versus , the Freundlich equilibrium constants were determined using the Freundlich equation's linear form. The n parameter measures the degree of nonlinear correlation between the concentration of a solution and the associated adsorption. Particularly, the adsorption process exhibits linearity when n is equal to 1. However, the adsorption process is categorised as chemical when n is less than 1, whereas it is categorised as physical when n is

greater than 1 (Vigdorowitsch et al. 2021). As seen in Table 3, the Freundlich equation produced a value of -4.9701 . In both instances, linear graphs were produced, demonstrating the applicability of these isotherms for the ongoing adsorption process.

Implementing isotherms, which are mathematical models that develop a link between the amount of adsorbate exist in the adsorbent material, is a common way to explain the adsorption mechanism (Serafin & Dziejarski 2023). Several isotherm models, such as the Langmuir and

Freundlich models, can describe the sectioning of metal ions between the phases of liquid and solid. According to the Langmuir isotherm model, adsorption takes place in a mono layer on a surface with a finite number of uniformly characterised adsorption sites, and the adsorbate does not migrate laterally across the surface (Abdelaziz et al. 2023). A site is incapable of further sorption after reaching its maximal sorption capacity. This indicates that the surface reaches a condition of saturation at which the maximum amount of adsorption that the surface is capable of is achieved.

PREDICTION OF ADSORBATE REMOVAL EFFICIENCY OR REQUIRED MASS ADSORBENT

The prediction contour was developed to simplify the estimation of phosphorus removal efficiency with various of phosphorus initial concentrations and the adsorbent mass needed. Based on the contour prediction, it can be observed from Figure 8 that the removal efficiencies are directly inversely correlated with the mass of adsorbents.

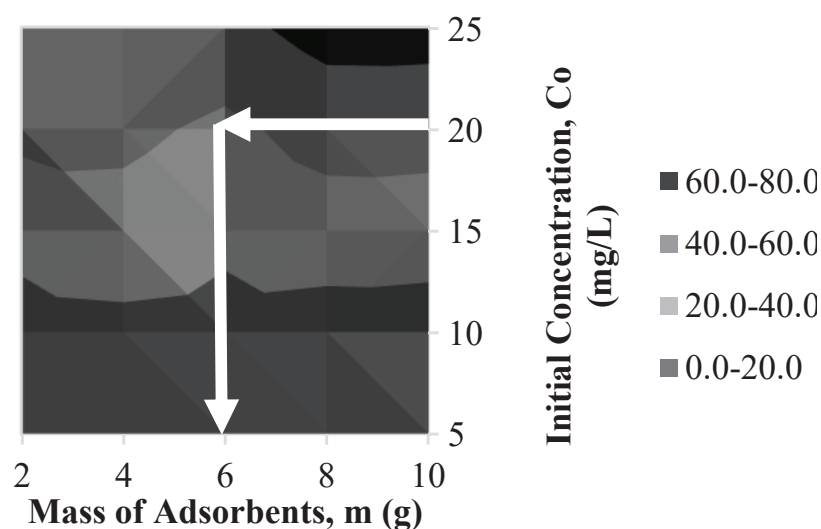


FIGURE 8. Contour diagram of removal efficiency on the removal of phosphate using marsh clam shells

Figure 8 shows the initial concentration is 20 mg/L of phosphorus, which can remove 20–40% of phosphorus with 6g of marsh clam shell. This contour can predict the removal and the adsorbent needed to further wastewater treatment (Chung et al. 2015). Figure 8 is helpful in immediately identifying the removal efficiency trend as a function of the initial adsorption circumstances, although there are exact values can be determined by precisely using the proposed equations. This is because such plots make it possible to comprehend the connection between removal efficiency and the initial adsorption conditions more clearly.

CONCLUSION

The current study assessed the effectiveness of marsh clam shells for phosphorus removal and showed that this type of waste adsorbent might be utilized effectively to eliminate phosphate from wastewater. Since precipitation

with carbonate is frequently implemented to eliminate phosphate from wastewater, marsh clam shell, primarily made of calcium, is a potentially ideal material for phosphorus adsorption. According to the batch test trials, all factors substantially impact the effectiveness of phosphate removal, but mass adsorbent has emerged as the crucial factor in this investigation. The experimental findings demonstrated that the increase in adsorbent mass increases the adsorbent particles' surface area and the percentage of phosphate removal. Specifically, with an adsorbent mass of 10 g, removal efficiencies of 78 % were achieved at an initial phosphorus concentration of 20 mg/L. This indicates that adsorbent dose increases lead to increased ion phosphorus removal, accelerating phosphorus removal from the aqueous solution. The study's goals were accomplished; marsh clam shells are high in calcium, and they may remove phosphate from wastewater. This study proves that the pseudo-first-order model proved greater results in phosphorus adsorption than the pseudo-second-order model. Meanwhile, Langmuir isotherm models

showed greater findings of phosphorus adsorption than Freundlich isotherm models, and this causes the Langmuir isotherm model to be the greatest model for phosphorus adsorption. This is evidenced by R^2 values obtained, with the pseudo-first-order model yielding an R^2 of 0.9951, indicating a strong fit to the data. Therefore, it may be inferred that waste adsorbent might be utilized more due to its efficiency as a cheap and accessible natural adsorbent. Marsh clam shells can encourage an ecologically beneficial method of acquiring a cleaner water supply while lowering the cost of wastewater treatment, particularly in eliminating phosphate.

ACKNOWLEDGEMENT

Communication of this research is made possible through monetary assistance by Universiti Tun Hussein Onn Malaysia and the UTHM Publisher's Office via Publication Fund E15216 and GPPS (Vot Q673).

DECLARATION OF COMPETING INTEREST

None.

REFERENCES

- Abdelaziz, M. A., Owda, M. E., Abouzeid, R. E., Alaysuy, O. & Mohamed, E. I. 2023. Kinetics, isotherms, and mechanism of removing cationic and anionic dyes from aqueous solutions using chitosan/magnetite/silver nanoparticles. *International Journal of Biological Macromolecules* 225:1462-1475.
- Abdullah, N. H., Azmi, M. A. M., Zaidi, M. A. M., Nasaruddin, N. B., Salim, N. A. A., Hairom, N. H. H., & Fulazzaky, M. A. 2024. Effect of Various Sizes of Calcined Marsh Clam Shell on Phosphate Removal from Aqueous Solution. *Journal of Advanced Research in Fluid Mechanics and Thermal Sciences* 113(1): 95-107.
- Abdullah, N. H., Xian, O. J., Yi, C. Z., Yuan, N. S., Yaacob, M. S. S., Salim, N. A. A. & Abdullah, F. 2023. Removal of phosphate from synthetic wastewater by using marsh clam (*Polymesoda expansa*) shell as an adsorbent. *Biointerface Res. Appl. Chem.* 3(1): 56.
- Alkurdi, S.S., Al-Juboori, R.A., Bundschuh, J., Bowtell, J. & Marchuk, A. 2021. Inorganic arsenic species removal from water using bone char: A detailed study on adsorption kinetic and isotherm models using error functions analysis. *Journal of Hazardous Materials* 405: 124112.
- Beretta-Blanco, A. & Carrasco-Letelier, L. 2021. Relevant factors in the eutrophication of the Uruguay River and the Río Negro. *Science of the Total Environment* 761: 143299.
- Boeykens, S.P., Piol, M.N., Legal, L.S., Saralegui, A.B. & Vázquez, C. 2017. Eutrophication decrease: phosphate adsorption processes in presence of nitrates. *Journal of Environmental Management* 203:888-895.
- Chung, H. K., Kim, W. H., Park, J., Cho, J., Jeong, T. Y., & Park, P. K. 2015. Application of Langmuir and Freundlich isotherms to predict adsorbate removal efficiency or required amount of adsorbent. *Journal of Industrial and Engineering Chemistry* 28: 241-246.
- Coates. J. 2000. Interpretation of infrared spectra, a practical approach. *Encyclopedia of analytical chemistry* 12:10815-10837.
- Ebrahiminezhad, A., Ghasemi, Y, Rasoul-Amini, S., Barar, J. & Davaran, S. 2013. Preparation of novel magnetic fluorescent nanoparticles using amino acids. *Colloids and Surfaces B: Biointerfaces* 102: 534-539.
- Feng, K., Deng, W., Zhang, Y., Tao, K., Yuan, J., Liu, J. & Hugueny, B. 2023. Eutrophication induces functional homogenization and traits filtering in Chinese lacustrine fish communities. *Science of The Total Environment* 857: 159651.
- Fetene, Y., & Addis, T. (2020). Adsorptive removal of phosphate from wastewater using Ethiopian rift pumice: batch experiment. *Air, Soil and Water Research*, 13, 1178622120969658.
- García-Zubiri, I. X., González-Gaitano, G. & Isasi, J. R. 2009. Sorption models in cyclodextrin polymers: Langmuir, Freundlich, and a dual-mode approach. *Journal of colloid and interface science* 337(11): 11-18.
- Hashim, K. S., Ewadh, H. M., Muhsin, A. A., Zubaidi, S. L., Kot, P., Muradov, M., ... & Al-Khaddar, R. (2021). Phosphate removal from water using bottom ash: Adsorption performance, coexisting anions and modelling studies. *Water Science and Technology*, 83(1), 77-89.
- Hussein, F. B., Cannon, A. H., Hutchison, J. M., Gorman, C. B., Yingling, Y. G., & Mayer, B. K. (2024). Phosphate-binding protein-loaded iron oxide particles: adsorption performance for phosphorus removal and recovery from water. *Environmental Science: Water Research & Technology*, 10(5), 1219-1232.
- Jiménez, B. 2005. Treatment technology and standards for agricultural wastewater reuse: a case study in Mexico. *Irrigation and Drainage: The journal of the International Commission on Irrigation and Drainage* 54(S1):S23-S33.

- Jing, K., Min, X., Song, W., Xu, D., & Li, X. (2024). Effect of filling materials on reconstructed soil phosphorus adsorption and desorption in mining area. *Soil and Tillage Research*, 235, 105895.
- Kesari, K.K., Soni, R., Jamal, Q. M. S., Tripathi, P., Lal, J. A., Jha, N. K. & Ruokolainen, J. 2021. Wastewater treatment and reuse: a review of its applications and health implications. *Water, Air, & Soil Pollution* 232:1-28.
- Kim, Y., Kim, D., Kang, S. W., Ham, Y. H., Choi, J. H., Hong, Y. P., & Ryoo, K. S. 2018. Use of powdered cockle shell as a bio-sorbent material for phosphate removal from water. *Bulletin of the Korean Chemical Society* 39(12): 1362-1367.
- Luo, D., Wang, L., Nan, H., Cao, Y., Wang, H., Kumar, T. V. & Wang, C. 2023. Phosphorus adsorption by functionalized biochar: A review. *Environmental Chemistry Letters* 21(1):497-524.
- Mekonnen, D. T., Alemayehu, E., & Lennartz, B. (2021). Adsorptive removal of phosphate from aqueous solutions using low-cost volcanic rocks: kinetics and equilibrium approaches. *Materials*, 14(5), 1312.
- Mishra, P., Singh, K., Dixit, U., Agarwal, A., & Bhat, R.A. 2022. Effective removal of 4-Aminophenol from aqueous environment by pea (*Pisum sativum*) shells activated with sulfuric acid: Characterization, isotherm, kinetics and thermodynamics. *Journal of the Indian Chemical Society* 99(7):100528.
- Mulkerrins, D.D.A.C.E., Dobson, A.D.W. & Colleran, E. 2004. Parameters affecting biological phosphate removal from wastewaters. *Environment international* 30(2):249-259.
- Nguyen, T. T. (2022). Effective removal of phosphate from waste water based on silica nanoparticles. *Journal of Chemistry*, 2022(1), 9944126.
- Oktor, K., Yuzer, N. Y., Hasirci, G., & Hilmioglu, N. (2023). Optimization of removal of phosphate from water by adsorption using biopolymer chitosan beads. *Water, Air, & Soil Pollution*, 234(4), 271.
- Penn, C., Chagas, I., Klimeski, A. & Lyngsie, G. 2017. A review of phosphorus removal structures: How to assess and compare their performance. *Water* 9(8): 583.
- Revellame, E. D., Fortela, D. L., Sharp, W., Hernandez, R. & Zappi, M. E. 2020. Adsorption kinetic modeling using pseudo-first order and pseudo-second order rate laws: A review. *Cleaner Engineering and Technology* 1:100032.
- Serafin, J. & Dziejarski, B. 2023. Application of isotherms models and error functions in activated carbon CO₂ sorption processes. *Microporous and Mesoporous Materials* 354(112513).
- Sharip, Z., Zaki, A.T., Shapai, M.A., Suratman, S. & Shaaban, A.J. 2014. Lakes of Malaysia: Water quality, eutrophication and management. *Lakes & Reservoirs: Research & Management* 19(2):130-141.
- Shimizu, S. & Matubayasi, N. 2023. Understanding Sorption Mechanisms Directly from Isotherms. *Langmuir* 39(17): 6113-6125.
- Tan, X., Gao, W., Duan, Z., Zhu, N., Wu, X., Ali, I. & Ruan, Y. 2023. Synthesis of novel algal extracellular polymeric substances (EPS)-based hydrogels for the efficient removal and recovery of phosphorus from contaminated waters: Development, characterisation, and performance. *Journal of Environmental Chemical Engineering* 11(1):109044.
- Vigdorowitsch, M., Pchelintsev, A., Tsygankova, L. & Tanygina, E. 2021. Freundlich isotherm: An adsorption model complete framework. *Applied Sciences* 11(17): 8078.
- Wu, S. C., Hsu, H. C., Hsu, S. K., Tseng, C. P., & Ho, W. F. 2017. Preparation and characterization of hydroxyapatite synthesized from oyster shell powders. *Advanced Powder Technology* 28(4):1154-1158.
- Wu, S. C., Hsu, H. C., Hsu, S. K., Tseng, C. P., & Ho, W. F. 2017. Preparation and characterization of hydroxyapatite synthesized from oyster shell powders. *Advanced Powder Technology* 28(4): 1154-1158.
- Xiong, J., Qin, Y., Islam, E., Yue, M. & Wang, W. 2011. Phosphate removal from solution using powdered freshwater mussel shells. *Desalination* 276(1-3):317-321.